Low energy band gap state in compressed needlelike structure of CdSb:Ni

T. R. Arslanov, R. G. Dzhamamedov, V. S. Zakhvalinskii, A. V. Kochura, V. V. Rodionov, and R. Ahuja

AFFILIATIONS

[1]Amirkhanov Institute of Physics, Daghestan Scientific Center, Russian Academy of Sciences (RAS), 367003 Makhachkala, Russia
[2]Department of Physics and Astronomy, Uppsala University, Box 516, Uppsala SE-75120, Sweden
[3]Department of Physics, Belgorod State University, RUS-308015 Belgorod, Russia
[4]South-West State University, Regional Centre of Nanotechnology, 50 Let Octjabrja Str. 94, 305040 Kursk, Russia

ABSTRACT

We studied the effect of high pressure on the border of intrinsic conductivity in CdSb doped with 0.5%Ni, the structure of which is needlelike due to spherical extended NiSb inclusions. The bandgap state has been found to be strongly governed by a structural transition in the composite structure. A pressure-induced phase exhibits an activation behavior only upon heating with a very low energy gap by 0.05 eV at 5.32 GPa, while metallic conductivity appears upon subsequent cooling, which is attributed to the instability of the cadmium antimonide structure. Room-temperature Hall effect measurements confirm that the high-pressure phase is not fully metallized, yielding a hole concentration of $4.08 \times 10^{18}\,cm^{-3}$ at the onset of structural transition and a reduced magnitude by order in this phase.

Intermetallic compounds based on cadmium antimonide, CdSb, demonstrate unique semiconducting properties that are of interest for application in high performance thermoelectric devices, including cooling or power generation technologies.[1] CdSb crystallizes into an orthorhombic structure (space group *Pbca*), and therefore, the electron transport should be strongly anisotropic. From the point of view of the electronic structure, the compound is a narrow-gap semiconductor with a bandgap of $E_g \sim 0.46$ eV at 297 K.[2,3] As a typical group II–V semiconductor, undoped cadmium antimonide has a *p*-type conductivity. However, *n*-type crystals can be obtained by doping In, Pb, Pd, etc. In the case of doping with transition metals such as Ni, Fe, and Mn, the *p*-type conductivity is conserved, since these impurities act as acceptors in the substituted structure. The result of such solubility demonstrates a diamagnetic response of the magnetic susceptibility.[4]

Recently, it has been shown that alloying by Ni, the CdSb compound leads to the formation of a needlelike structure due to the formation of nanoscale oriented spheroidal $Ni_{1-x}Sb_x$ clusters with a high aspect ratio of $m = l/r$ (where l and r are the half-lengths of the major and minor axes, respectively). The bulk compound of $Ni_{1-x}Sb_x$ is known as a ferromagnet at concentration $x < 7.5\%$.[5] Remarkably, in the form of NiSb nanoclusters, the CdSb-NiSb system exhibits not only high temperature ferromagnetic order with $T_C > 300$ K[6] but also the low-temperature hopping conductivity with variable range hopping ($\sim \exp[T_0/T)^{\xi}]$ of Mott ($\xi = 1/4$) or Efros-Shklovskii type ($\xi = 1/2$).[7] In particular, it was found that in the region of the metal to insulator transition between $T \sim 5$ and 20 K, the predominance of the above-noted activation regimes strongly correlates with the concentration of the magnetic impurity. Despite the extensive study of transport properties in Ni-doped CdSb below 300 K (Refs. 7 and 8), a question related to the effect of the Ni impurity on the fundamental energy gap remains unclear. Moreover, the values of E_g even for the CdSb compound vary in the range of 0.44–0.57 eV based on the available experimental and theoretical results.[2,3,9–11] In this regard, high pressure may be the convenient parameter, which allows one to understand the evolution of E_g in this material.

In this Letter, we measured the temperature dependence of resistivity in the region of intrinsic conductivity of the CdSb-NiSb system at high pressure $P < 6$ GPa in order to probe E_g behavior as well as the effect of structural transition on the electronic transport. As shown for *p*-CdSb doped with 0.5% Ni, a pressure-induced phase is not completely metallized compared to that previously suggested for the CdSb compound from the high-pressure X-ray diffraction (XRD) study.[12] Instead, we find the presence of a very low energy gap with $E_g \sim 0.05$ eV, which may

develop a possible scenario for the topological semimetallic state in compressed CdSb:Ni.

Single crystals of CdSb doped with 0.5% Ni were obtained by the modified Bridgman method upon slow cooling in a constant temperature gradient. Initially, Ni was dissolved in Cd in a melt heated to 700 °C for 8 h. Then, stoichiometric amounts of Sb (purity 99.999%) and Cd:Ni were placed in a graphitized quartz ampule filled after pumping out Ar gas at a pressure of $P = 0.1$ atm. After sealing the ampoule, the material was kept at a temperature of 460 °C for 12 h, and then the ampoule was cooled with a rate of 0.5 °C per hour. According to XRD, the CdSb single crystal matrix had an orthorhombic structure with the same parameters as undoped CdSb. The lattice parameters for CdSb doped with 0.5% Ni correspond to $A = 6.492$ (8) Å, $b = 8.268$ (6) (Å), and c = 8.512 (7) (Å). The growth direction of the ingots deviated by an angle of $50 \pm 5°$ from the crystalline axis [100]. As followed from scanning electron microscopy (SEM), the samples contained bulk structural defects in the form of nonextended (up to several μm) cracks and cavities with lateral sizes of up to 5 μm. depicts the SEM image for the sample with 0.5% Ni, where the NiSb clusters appear in the form of spherical extended inclusions of ~30–40 μm and with a diameter of up to ~5 μm.

DC resistivity and Hall effect measurements were performed using a six-contact method in a Toroid type high pressure apparatus under hydrostatic pressure at room temperature. Temperature-dependent DC resistivity measurements were carried out in the range of 160–360 K and pressures up to $P \sim 5.32$ GPa using a special type of tungsten-cobalt punch. As a pressure cell, the Teflon capsule with a working volume of ~80 mm^3 equipped by 8–12 lead-in contacts was used. The capsule configuration allowed us to simultaneously measure the resistivity and Hall effect under pressure at room temperature conditions. The samples were $2.8 \times 1.1 \times 1.1$ mm^3 in dimensions. A pure mixture of ethanol-methanol with the ratio of 4:1 was used as a pressure-transmitting medium. The pressure inside the Teflon cell was continuously monitored by a manganin wire and calibrated on the end points to the Bi phase transition.

shows the temperature dependences of the resistivity $\rho(T)$ at pressures up to 2.46 GPa (a) and 5.32 GPa (b). At ambient

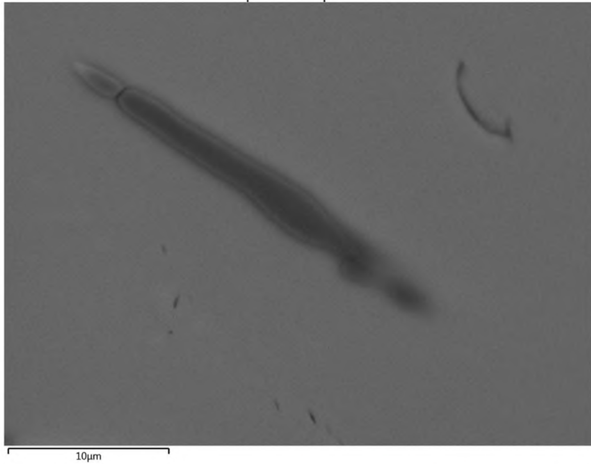

FIG. 1. SEM image of a CdSb-NiSb needlelike structure.

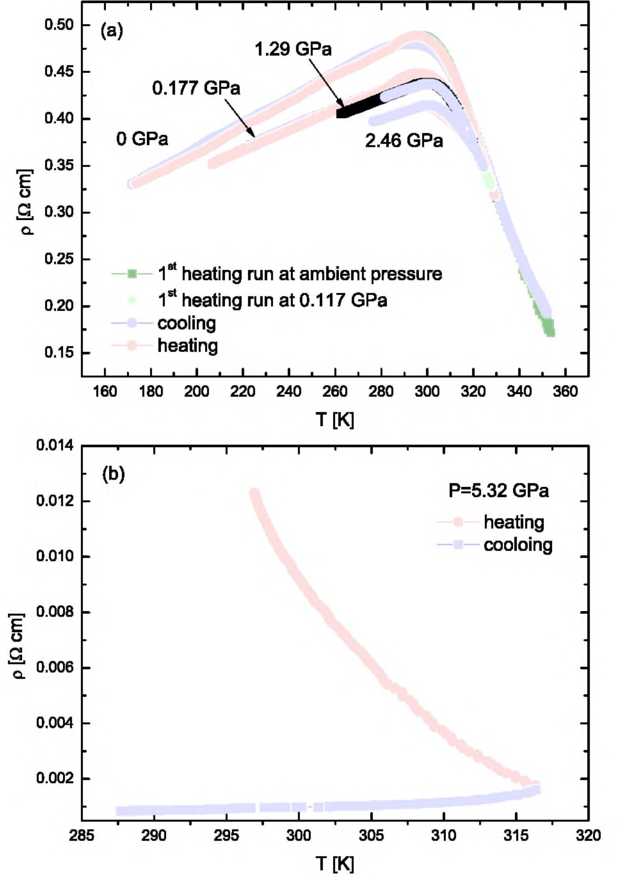

FIG. 2. Temperature dependence of resistivity for CdSb-NiSb during heating and cooling collected at various pressures: (a) 0–2.46 GPa and (b) 5.32 GPa.

pressure, the dependence of $\rho(T)$ exhibits a maximum at T^{max} ~ 295 K [ ] associated with the metal to semiconductor transition. The metallic type of conductivity below 295 K is typical for CdSb:Ni compounds and characterized by a region of impurity conductivity. With the pressure application, T^{max} begins to shift to high temperatures with an average rate of $dT/dP \sim 2.5$ K/GPa, indicating a positive sign of the pressure coefficient. At a pressure of 5.32 GPa [ ], a significant decrease in resistivity is predominant, associated with a structural change in CdSb. Indeed, the dependence of $\rho(P)$ measured at room temperature shows a sharp decrease by almost two orders of magnitude near $P = 3$ GPa, as is shown in . In addition, there is a noticeable hysteresis behavior during decompression, which is commonly attributed to the first order structural transformation. However, this transformation cannot be classified as a reversible structural transition, since the value of $\rho(P)$ at decompression does not return to the initial value $\rho_0 = 0.23$ Ω cm at $T = 295$ K.

The bulk CdSb is known as a compound that demonstrates the number of unique phenomena under pressure, including phase transformations, new phase formations, pressure decomposition, and amorphization after decompression. Thus, the observed behavior of $\rho(T)$ in our sample can be explained as the formation of the pressure decomposition of Sb + Cd in the high-pressure region, i.e., irreversible

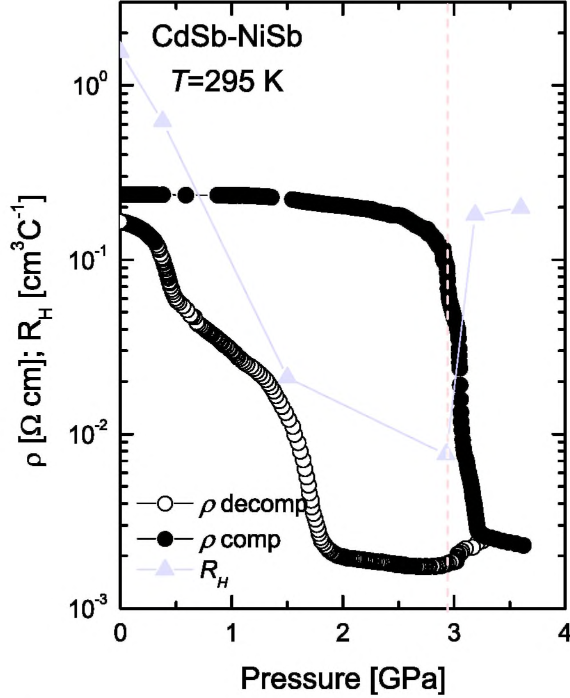

FIG. 3. Pressure dependence of resistivity and the Hall coefficient measured at room temperature. Solid symbols mean the compression, while open symbols denote the decompression. The dashed line corresponds to the onset of structural transition. The data for R_H are divided by a factor of 2000.

phase transformation upon cooling after the initial heating. The irreversible hysteretic behavior of $\rho(P)$ after decompression also indicates the pressure instability of the Ni-doped structure ( ). As described in Ref. , the structural change of the orthorhombic phase occurs above 7.3 GPa with the formation of a two-phase mixture of a simple hexagonal phase and a hexagonal close-packed phase of Cd. The dependence of $\rho(P)$ for Ni-doped CdSb also reflects the structural transition, which undergoes at lower pressures of $P \sim 3$ GPa. This circumstance can be explained as follows: the availability of NiSb needles leads to a weakening of bond lengths in the crystal structure of CdSb with a shift of the structural transition point toward lower pressures. In particular, a similar situation is reported for some of the Mn-doped chalcopyrite materials.

Earlier, it was found that the phase transformation at 7 GPa in oriented CdSb crystals is accompanied by the transition of the semiconductor to metal as shown by the electrical transport measurements. Furthermore, the metallic conductivity was attributed to an amorphous phase at decompression. An appearance of the amorphous metallic phase occurs due to the pressure decomposition of the semiconducting stoichiometric composition and an excess of Cd. Based on these considerations, the structural transition to the metallized high-pressure phase ($P = 5.23$ GPa) should lead to $E_g \rightarrow 0$, i.e., complete overlapping of the top of a valence band with the bottom of a conductivity band. In our case, the unusual behavior of $\rho(T)$ lies in the fact that during the structural transition, the activation type of conductivity in the new phase is preserved only upon heating, while a metallic regime predominates under cooling [ ]. This implies the thermal instability of the compressed compound, and, hence, the observed metallic conductivity should be closely related to the amorphization of the decomposed composition. Interestingly, the reverse run of the hysteresis depicted from resembles several pressure-dependent phase transitions. In this regard, it can be assumed that amorphization is only partial in conjunction with the crystalline phase of Cd, which tends to recover as pressure decreases.

On the other hand, the pressure dependence of the Hall coefficient $R_H(P)$ measured in the field $H = 2$ kOe suggests an increase in the Hall concentration of charge carriers in approximation to the structural transition region ( ). The coefficient $R_H = 1/ep$ is assumed to be mainly related to the activation of holes in the valence band. The initial concentration calculated in this way is $p = 2.015 \times 10^{16}$ cm^{-3}, which is in agreement with data of Laiho *et al.* With increasing pressure, p increases by almost two orders of magnitude with a value of 4.08×10^{18} cm^{-3} at $P \sim 2.93$ GPa, with a further decrease by order. This supports that the transformed phase of the CdSb-NiSb system does not have a simple topology of the band structure, and the high-pressure phase cannot be itself considered as completely metallized.

In order to determine the pressure dependence of the bandgap, the high-temperature regions of conductivity $\sigma = 1/\rho$ as a function of $1/T$ are plotted, as shown in . Here, linear sections (straight lines in the figure) correspond to the activation law of $\sigma = \sigma_0 \exp(E_g/2k_BT)$, while the dependence of $E_g(P)$ is shown in . Given that the variation in ρ(T) undergoes almost linearly up to higher temperatures, a slope of the fitting line remains the same within a specified temperature range. It allowed us to reliably extract the values of E_g at each of the pressures. Thus, experimentally determined $E_g = 0.35$ eV at $P = 0$ GPa for CdSb-NiSb, which is noticeably lower than the value of 0.46 eV for pure CdSb. As can be seen, the dependence of $E_g(P)$ demonstrates an almost monotonic decrease with increasing pressure, reaching a value of 0.05 eV at $P = 5.23$ GPa. In this case, the rate dE_g/dP changes from -0.088 eV/GPa in the interval of $P = 0$–2.46 GPa to -0.017 eV/GPa in $P = 2.46$–5.23 GPa.

Based on *ab initio* band structure calculations of CdSb, the bandgap $E_g = 0.44$ eV has been found to be indirect with an absolute maximum of the valence band located near the point X of the Brillouin zone in the $\Sigma(\Gamma\text{-}X)$ direction. For the direct gap, the smallest transition was found at the point Γ (Γ_4-Γ_5), which is 2.18 eV,

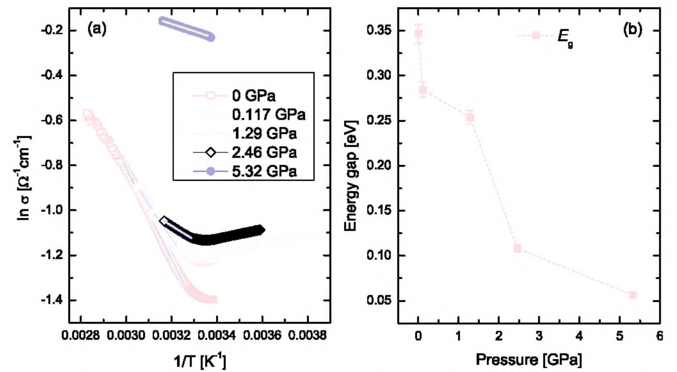

FIG. 4. (a) Dependence of logarithmic $\sigma = 1/\rho$ as a function of $1/T$. (b) Variation of E_g vs pressure.

which allowed by the selection rules. Therefore, a value of 0.35 eV defined for CdSb-NiSb from the resistivity measurements is most likely related to an indirect bandgap. The observation of such a low energy gap of 0.05 eV with an increasing pressure may indicate the evolution of a band structure with a quite good permission for a topological phase transition. Surprisingly, the possible topological transition in the Ni-doped CdSb is triggered by a structural transformation, since its existence is believed to be hindered or separated by the structural transition. A general trend for the pressure-induced topological electronic state proceeds with the reopening of the bandgap and its further increase with increasing pressure. For instance, a similar situation has been demonstrated for 3D Dirac or Weyl semimetals. We would also like to notice that the electrical conductivity in the pressure-induced phase may be enhanced due to the additional contribution from sizable NiSb inclusions, which are metallic in nature. Thus, it is reasonable to expect that their electronic and magnetic states have a direct relation to the observed energy gap. A more detailed study of E_g in the transformed phase by means of a combination between optical methods and higher pressures than explored in the current work is highly required.

In summary, based on the high-pressure electronic transport measurements, we have found a structural change in the CdSb-NiSb composite, which has been accompanied by a phase formation with a low-energy gap of 0.05 eV. Moreover, this pressure-induced phase is unstable and exhibits a metallic conductivity only upon cooling. Such a behavior indicates the pressure-induced decomposition of the CdSb host with a partial amorphization of the compound after decompression. The observation of a low energy bandgap opens up prospects for searching a topological semimetallic state in compressed Ni-doped CdSb.

This work was supported by the Russian Foundation for Basic Research, Research Project No. 19-02-00031, and the RAS Program # 4. The research work of T.R.A. at Uppsala University was supported by the Swedish Institute under Visby programme scholarship (No. 25908/2018). The financial support from the Ministry of Education and Science of the Russian Federation (Grant No. 16.2814.2017/ПЧ) is acknowledged.

REFERENCES

[1] S. Wang, J. Yang, L. Wu, P. Wei, J. Yang, W. Zhang, and Y. Grin, **27**, 1071–1081 (2015).
[2] W. J. Turner, A. S. Fischler, and W. E. Reese, **121**, 759 (1961).
[3] W. J. Turner, A. S. Fischler, and W. E. Reese, **32**, 2241 (1961).
[4] M. Matyáš and M. Klígl, **18**, 376 (1968).
[5] K. Hoselitz, *Ferromagnetic Properties of Metals and Alloys* (Clarendon, Oxford, 1952).
[6] R. Laiho, A. V. Lashkul, E. Lähderanta, K. G. Lisunov, I. Ojala, and V. S. Zakhvalinskii, **300**, e8–e11 (2006).
[7] R. Laiho, A. V. Lashkul, K. G. Lisunov, E. Lähderanta, M. A. Shakhov, and V. S. Zakhvalinskii, **20**, 295204 (2008).
[8] R. Laiho, A. V. Lashkul, K. G. Lisunov, E. Lähderanta, M. A. Shakhov, and V. S. Zakhvalinskii, **70**, 428–432 (2009).
[9] D. M. Bercha, I. V. Slipukhina, M. Sznajder, and K. Z. Rushchanskii, **70**, 235206 (2004).
[10] Y. Yomada, **35**, 1600–1607 (1973).
[11] E. K. Arushanov, **13**, 1 (1986).
[12] V. F. Degtyareva, O. Degtyareva, H. Mao, and R. J. Hemley, **73**, 214108 (2006).
[13] K. E. Almin, **4**, 400–407 (1948).
[14] L. G. Khvostantsev, V. N. Slesarev, and V. V. Brazhkin, **24**, 371 (2004).
[15] R. Laiho, A. V. Lashkul, K. G. Lisunov, E. Lähderanta, M. A. Shakhov, and V. S. Zakhvalinskii, **6**, 1328–1331 (2009).
[16] A. Y. Mollaev, R. K. Arslanov, R. G. Dzhamamedov, S. F. Marenkin, and S. A. Varnavskii, **41**, 217 (2005).
[17] R. G. Dzhamamedov, A. Ju. Mollayev, A. V. Kochura, P. V. Abakumov, R. K. Arslanov, S. F. Marenkin, and M. B. Dobromyslov, J. Nano-Electron. Phys. 7(4), 04088 (2015).
[18] R. G. Dzhamamedov, T. R. Arslanov, A. Y. Mollaev, and A. V. Kochura, **699**, 1104–1107 (2017).
[19] A. Y. Mollaev, I. K. Kamilov, R. K. Arslanov, T. R. Arslanov, U. Z. Zalibekov, V. M. Novotortsev, S. F. Marenkin, and V. M. Trukhan, **100**, 202403 (2012).
[20] T. R. Arslanov, A. Y. Mollaev, I. K. Kamilov, R. K. Arslanov, L. Kilanski, V. M. Trukhan, T. Chatterji, S. F. Marenkin, and I. V. Fedorchenko, **103**, 192403 (2013).
[21] R. Arslanov, A. Mollaev, I. Kamilov, T. Arslanov, U. Zalibekov1, V. Novotortsev, S. Marenkin, and I. Troyanchuk, **250**, 736–740 (2013).
[22] M. K. Tran, J. Levallois, P. Lerch, J. Teyssier, A. B. Kuzmenko, G. Autès, O. V. Yazyev, A. Ubaldini, E. Giannini, D. van der Marel, and A. Akrap, **112**, 047402 (2014).
[23] M. Zhang, X. Wang, A. Rahman, Q. Zeng, D. Huang, R. Dai, Z. Wang, and Z. Zhang, **112**, 041907 (2018).
[24] R. Juneja, R. Shinde, and A. K. Singh, **9**, 2202–2207 (2018).
[25] S. Khalid, F. P. Sabino, and A. Janotti, **98**, 220102(R) (2018).
[26] Y. Li, C. An, C. Hua, X. Chen, Y. Zhou, Y. Zhou, R. Zhang, C. Park, Z. Wang, Y. Lu, Y. Zheng, Z. Yang, and Z. Xu, **3**, 58 (2018).
[27] Y. A. Sorb, V. Rajaji, P. S. Malavi, U. Subbarao, P. Halappa, S. C. Peter, S. Karmakar, and C. Narayana, **28**, 015602 (2016).
[28] X. Li, D. Chen, M. Jin, D. Ma, Y. Ge, J. Sun, W. Guo, H. Sun, J. Han, W. Xiao, J. Duan, Q. Wang, C. Liu, R. Zou, J. Cheng, C. Jin, J. Zhou, J. B. Goodenough, J. Zhu, and Y. Yao, **116**(36), 17696–17700 (2019).
[29] S. Zhang, Q. Wu, L. Schoop, M. N. Ali, Y. Shi, N. Ni, Q. Gibson, S. Jiang, V. Sidorov, W. Yi, J. Guo, Y. Zhou, D. Wu, P. Gao, D. Gu, C. Zhang, S. Jiang, K. Yang, A. Li, Y. Li, X. Li, J. Liu, X. Dai, Z. Fang, R. J. Cava, L. Sun, and Z. Zhao, **91**, 165133 (2015).
[30] S. Güler-Kılıc and Ç. Kılıc, **94**, 165203 (2016).